

## Research Paper

**Cite this article:** Villora-Montero M, Pérez-del-Olmo A, Valmaseda-Angulo M, Raga JA, Montero FE (2023). The genus *Microcotyle* in Mediterranean scorpaenoids (Teleostei), including the description of *Microcotyle merche* n. sp. from *Helicolenus dactylopterus* (Delaroche, 1809). *Journal of Helminthology* **97**, e25, 1–15. <https://doi.org/10.1017/S0022149X23000019>

Received: 29 November 2022

Revised: 4 January 2023

Accepted: 4 January 2023

### Keywords:


New host; Sebastidae; Scorpaenidae; *Microcotyle algeriensis*; *Microcotyle sebastis*; haptor morphology

### Author for correspondence:

M. Villora-Montero,

E-mail: [maria.villora@uv.es](mailto:maria.villora@uv.es)

# The genus *Microcotyle* in Mediterranean scorpaenoids (Teleostei), including the description of *Microcotyle merche* n. sp. from *Helicolenus dactylopterus* (Delaroche, 1809)

M. Villora-Montero , A. Pérez-del-Olmo, M. Valmaseda-Angulo, J.A. Raga and F.E. Montero

Marine Zoology Unit, Cavanilles Institute of Biodiversity and Evolutionary Biology, Science Park, University of Valencia, C/Catedrático José Beltrán 2, 46980 Paterna, Spain

## Abstract

More than 65 species of the genus *Microcotyle* Van Beneden & Hesse, 1863, have been described to date, most of them infecting Perciformes. Among the scorpaenoids (Perciformes, formerly Scorpaeniformes) the species of the genus *Microcotyle* parasitize sebastids and scorpaenids worldwide. In this study, we provide new morphological and molecular data for *Microcotyle* spp. in sebastids and scorpaenids from the Western Mediterranean and north-east Atlantic. Specimens of *Helicolenus dactylopterus* (Delaroche, 1809) ( $n = 107$ ) and *Scorpaena* spp. ( $n = 107$ ) were examined and their microcotylid specimens morphologically and molecularly characterized. *Microcotyle merche* n. sp. ex *H. dactylopterus* and specimens of *Microcotyle algeriensis* Ayadi, Gey, Justine & Tazerouti, 2016 from a new host and locality (*Scorpaena scrofa* from the north-east Atlantic) are herein described. Both species are phylogenetically close, but their morphology is markedly different mostly because the anterior lobe of the haptor present in other *Microcotyle* species is almost absent in *M. algeriensis*. Findings of *M. merche* n. sp. in the Mediterranean also excludes the presence of *Microcotyle sebastis* in this sea, encouraging the review of the exceptionally large host range and geographical distribution of this species.

## Introduction

*Microcotyle* Van Beneden & Hesse, 1863 is one of the most frequent and diverse monogenean genera, with 67 species listed in the World Register of Marine Species (2022). This diversity implies a high taxonomic complexity, and as a consequence of *Microcotyle* being the first microcotylid genus erected, many species were initially assigned to this taxon. Most species were subsequently reassigned to new genera (see Mamaev, 1986; World Register of Marine Species, 2022), but many citations still need revision. The diversity of *Microcotyle* is also reflected in the host range, with the parasites infecting several species of different fish orders, mostly Eupercaria and Perciformes (formerly belonging to Perciformes and Scorpaeniformes, respectively, see World Register of Marine Species, 2022). Among various host families, species of *Microcotyle* (13.4%) have mostly been reported in sparids (Eupercaria), mainly in the Mediterranean (see also Lablack *et al.*, 2022). Within the Scorpaenoidei (Perciformes), 7.5% of *Microcotyle* species have been reported in sebastids and 3% in scorpaenids (Gibson *et al.*, 2006; Ayadi *et al.*, 2017; Ono *et al.*, 2020; only including reports identified up to species level). To date, these records are mostly from the Pacific Ocean, but also from the Atlantic Ocean and the Mediterranean Sea.

The great morphological resemblance between *Microcotyle* species requires the exploration of new morphological characters to differentiate at species level. For example, based on their similarity, several specimens of *Microcotyle* spp. from numerous hosts worldwide have been identified as *Microcotyle sebastis* or *Microcotyle erythrini*, but many of these records have been considered as doubtful, often revised and reclassified in different species (e.g. Ayadi *et al.*, 2017; Bouguerche *et al.*, 2019b; Villora-Montero *et al.*, 2020). There is an additional need to expand the molecular database and define the genome regions and distance ranges useful for differentiating species. This study provides the description of specimens found in a recent study on scorpaenoids of commercial interest (*Helicolenus dactylopterus* (Delaroche, 1809) and *Scorpaena* spp.) from the Mediterranean and north-east Atlantic. The descriptions include a new species of *Microcotyle* and a new host and locality records for *Microcotyle algeriensis*. These new findings contribute to the knowledge about the diversity of this parasite genus, which is particularly abundant in the study area, specially in scorpaenoid hosts.

© The Author(s), 2023. Published by Cambridge University Press. This is an Open Access article, distributed under the terms of the Creative Commons Attribution licence (<http://creativecommons.org/licenses/by/4.0/>), which permits unrestricted re-use, distribution and reproduction, provided the original article is properly cited.

## Materials and methods

### Sample collection

A total of 107 *H. dactylopterus* (Sebastidae) and 107 *Scorpaena* spp. (*Scorpaenidae*: 37 *Scorpaena notata* Rafinesque, 1810, 42 *Scorpaena porcus* L. and 28 *Scorpaena scrofa* L.) were examined for microcotylid infections. Fishes were collected by commercial bottom trawling vessels during the period 2015–2016, off Guardamar del Segura (Balearic, Division 37.1.1, Western Mediterranean Sea), and Galicia (Bay of Biscay-South, Division 27.8.c, north-east Atlantic) (see [table 1](#) for the biological and geographical data of samples; fishing areas reported according to the United Nations Food and Agriculture Organization, <https://www.fao.org/fishery/en/area/search>). Fish were stored on ice and transferred to the laboratory (Cavanilles Institute of Biodiversity and Evolutionary Biology) where they were weighed and measured (weight provided in g and standard length in cm, expressed as the range with the mean and standard deviation in parentheses; this information is only provided for infected hosts in the parasite description sections). Fish were dissected fresh and the gills were examined for monogeneans under a stereomicroscope. All specimens were collected and washed in 0.9% saline solution. Two different protocols described in Villora-Montero *et al.* (2020) were used for the fixation and storage of mature specimens of *Microcotyle* spp. Firstly, with specimens selected for molecular analyses, the testes and clamps were counted in temporary saline solution preparations and then the entire worms were photographed prior to excising the specimens into three parts. The anterior and posterior parts were kept as molecular vouchers (hologenophores *sensu* Pleijel *et al.*, 2008) and the middle part of the body was used for DNA extraction (the latter material was preserved in molecular-grade ethanol). In the second protocol, used for morphological analyses, representative specimens (not broken, contracted, stretched, wrinkled or folded) were selected, fixed in 4% formaldehyde solution for four days and preserved in 70% ethanol. The prevalence, expressed as a percentage, was calculated as the number of infected fish divided by the total number of analysed fish, and mean intensity, expressed as the mean  $\pm$  standard deviation (SD), was calculated as the number of monogenean specimens collected in infected hosts divided by the number of fish infected, following Bush *et al.* (1997).

### Morphological analyses

Selected parasites were stained with iron-acetocarmine, dehydrated through an ethanol series (70–100%), cleared with

dimethyl phthalate and examined as permanent mounts in Canada balsam under a Nikon Optiphot-2 light microscope (Nikon Instruments, Tokyo, Japan) with differential interference contrast at magnifications of 40–1000 $\times$ .

Clamps, testes and spines were counted, and all morphometric measurements were taken from illustrations made with a drawing tube attached to the Nikon Optiphot-2 light microscope. The illustrations were digitalized to obtain 46 morphometric measurements (in micrometres, see [table 2](#)) using ImageJ v.1.48 software (Schneider *et al.*, 2012). Morphometric data are reported as mean  $\pm$  SD in the description, and as ranges in tables (see [tables 2, 3](#)). Clamp terminology follows Llewellyn (1956) (see [fig. 1](#)). Following the suggestions of Villora-Montero *et al.* (2020) to differentiate *Microcotyle* species, the lengths of the anterior and posterior haptor lobes and the thickness of clamps presented by the ratio between 'C' sclerite maximum width/total clamp length are provided. A total of 59 specimens of *Microcotyle* spp. were selected and drawn:  $n = 40$  ex *H. dactylopterus* ( $n = 20$  from the Western Mediterranean Sea and  $n = 20$  from the north-east Atlantic) and  $n = 19$  ex *S. scrofa* from the north-east Atlantic (no microcotylids were found in Mediterranean samples). No infected *S. notata* and *S. porcus* were found. Type-specimens were deposited in the Collection of the Natural History Museum (NHMUK), London, UK.

### Molecular methods

Genomic DNA isolation from the middle part of the body of the specimens was performed with Chelex<sup>TM</sup>100 Resin (BIO-RAD, Hercules, USA) following the protocol described in Lablack *et al.* (2022). Partial fragments of the mitochondrial cytochrome *c* oxidase subunit 1 gene (*cox1*) were amplified using the primers JB3 (=COI-ASmit1) (forward: 5' -TTT TTT GGG CAT CCT GAG GTT TAT-3') and JB4.5 (= ASmit2) (reverse: 5'-AAA GAA AGA ACA TAA TGA AAA TG-3') (Bowles *et al.*, 1995). The thermocycling profile consisted of an initial denaturation step at 94°C for 5 min, followed by 40 cycles of amplification (92°C for 30 s, 45.5°C for 45 s, and 72°C for 90 s) and a final extension step at 72°C for 10 min. Polymerase chain reaction (PCR) amplicons were purified using the QIAquick<sup>TM</sup> PCR Purification Kit (Qiagen Ltd., Hilden, Germany) following the manufacturer's instructions and both strands were sequenced directly using the PCR primers. Sequencing was carried out at Macrogen Europe Inc. (Amsterdam, the Netherlands).

Contiguous sequences were assembled using MEGA v.6 (Tamura *et al.*, 2013) and alignments were constructed using

**Table 1.** Summary of the sampling data and biological parameters of the scorpaenoid fishes examined.

	Locality	N	TL	SL	W
<i>Helicolenus dactylopterus</i>	Western Mediterranean	74	30.5 $\pm$ 1.4	25.1 $\pm$ 1.0	415.9 $\pm$ 67.6
	Bay of Biscay (Atlantic)	33	17.4 $\pm$ 03.4	14.3 $\pm$ 2.8	92.6 $\pm$ 64.8
<i>Scorpaena scrofa</i>	Western Mediterranean	9	32.3 $\pm$ 4.7	25.7 $\pm$ 3.7	621.8 $\pm$ 219.3
	Bay of Biscay (Atlantic)	19	32.6 $\pm$ 3.8	25.4 $\pm$ 2.8	514.6 $\pm$ 141.3
<i>Scorpaena porcus</i>	Western Mediterranean	34	15.1 $\pm$ 4.1	15.0 $\pm$ 19.6	83.8 $\pm$ 95.2
	Bay of Biscay (Atlantic)	8	18.25 $\pm$ 5.9	14.5 $\pm$ 4.8	149.9 $\pm$ 125.9
<i>Scorpaena notata</i>	Western Mediterranean	37	14.2 $\pm$ 2.1	11.01 $\pm$ 1.9	52.5 $\pm$ 21.2

Abbreviations: N, number of individual fish examined; TL, total length (cm); SL, standard length (cm); W, weight (g).

**Table 2.** Metrical ranges for *Microcotyle merche* n. sp. from *Helicolenus dactylopterus* and *Microcotyle algeriensis* from *Scorpaena* spp. Records from present and other studies.

Host species	<i>Microcotyle merche</i> n. sp.				<i>Microcotyle algeriensis</i>	
	<i>Helicolenus dactylopterus</i>				<i>Scorpaena scrofa</i>	<i>Scorpaena notata</i>
	Present study		Ayadi <i>et al.</i> 2017	Radujković & Euzet, 1989	Present study	Ayadi <i>et al.</i> 2017
Source	Western Mediterranean	Bay of Biscay	Western Mediterranean	Central Mediterranean	Bay of Biscay	Western Mediterranean
United Nations Food and Agriculture Organization Fishing Area	Western Mediterranean	Bay of Biscay	Western Mediterranean	Central Mediterranean	Bay of Biscay	Western Mediterranean
body length	2517.2–5345.1	3009.6–5706.0	410–3800	2500–3200	2298.1–5163.0	1900–4300
body width	422.2–887.5	380.5–787.4		500–600	427.0–780.2	300–860
width at sucker level	88.5–198.6	163.2–243.4			144.2–215.6	
width at genital atrium level	170.6–405.3	249.9–416.6			245.3–358.9	
width at testes level	262.8–706.1	190.8–533.8			301.4–589.6	
body length without haptor	1613.1–4479.3	2084.7–5706.0			1879.0–4614.6	
haptor length	838.5–1360.4	625.3–1719.3	570–1200		329.3–957.9	450–1040
haptor anterior lobe length	196.5–483.7	173.4–546.1			89.5–250.7	
minimum width at peduncle	141.4–478.5	114.5–406.4			177.8–839.2	
number of clamps	42–58	48–60	49–58	38–56	22–34	20–39
maximum clamp length	38.4–57.4	42.8–60.8	42–74		34.7–56.7	48–85
maximum clamp width	58.0–78.0	74.9–91.4	40–69		63.8–81.6	40–78
maximum clamp length	38.4–57.4	42.8–60.8	42–74		34.7–56.7	48–85
maximum clamp width	58.0–78.0	74.9–91.4	40–69		63.8–81.6	40–78
anterior clamp length	27.2–45.4	32.4–47.9			34.5–52.9	
anterior clamp width	52.3–77.5	62.5–89.7			49.5–76.6	
posterior clamp length	30.0–42.0	38.3–55.2			33.0–46.7	
posterior clamps width	43.5–68.5	58.1–87.7			49.4–65.9	
sclerite 'c' width	4–7	4–9			2–6	
sucker length	35.8–79.8	59.4–92.6	47–73		52.8–72.4	40–85
sucker width	34.0–77.7	60.9–90.1			54.4–77.8	39–76
pharynx length	31.1–74.1	63.1–77.9	40–77		53.2–87.4	50–100
pharynx width	31.3–72.8	53.9–82.0	50–69		58.3–86.2	46–90
oesophagus length	154.1–443.0	279.0–598.3			254.0–381.6	
testes to anterior end distance	1206.1–2692.7	1347.9–4172.8			1526.4–2179.2	
number of testes	13–18	14–22	10–17	15–17	10–17	9–20
number of testis rows	1–2	1–2			1–2	
testes length	48.6–126.5	54.9–95.2			44.6–77.4	
testes width	43.7–147.9	50.8–114.6			56.8–88.6	
testicular area length	308.0–923.4	339.4–907.8			351.7–584.6	600–900
testicular area width	108.8–891.6	121.4–938.4			66.3–179.3	500–750
genital atrium to anterior end distance	143.3–844.4	196.5–341.3	270–520		251.2–365.2	110–400
genital atrium length	94.6–265.6	167.3–300.7	95–160	170	120.9–209.0	77–175
genital atrium width	128.1–307.8	174.0–323.9	102–150	95	129.5–266.4	83–130
number of spines in main chamber of the genital atrium	146–221	163–212	104–307		189–234	68–162
length of spines in main chamber of the genital atrium	4–8	6–10			6–9	

(Continued)

Table 2. (Continued.)

Host species	<i>Microcotyle merche</i> n. sp.				<i>Microcotyle algeriensis</i>	
	<i>Helicolenus dactylopterus</i>				<i>Scorpaena scrofa</i>	<i>Scorpaena notata</i>
	Present study		Ayadi et al. 2017	Radujković & Euzet, 1989	Present study	Ayadi et al. 2017
United Nations Food and Agriculture Organization Fishing Area	Western Mediterranean	Bay of Biscay	Western Mediterranean	Central Mediterranean	Bay of Biscay	Western Mediterranean
number of spines in pockets of the genital atrium	20–38	28–40	18–38		18–38	8–18
length of spines in pockets of the genital atrium	6–10	9–14			8–11	
copulatory organ length	41.5	41.2–85.3			39.6–55.0	
copulatory organ width	43.1	21.6–71.4			47.6–57.6	
germarium to anterior end distance	1129.4–2077.0	1257.6–2345.4			1421.8–2075.2	
vagina to anterior end distance	618.4–1452.0				238.5	
germarium length	547.3–1405.9	535.9–1.131.0			538.3–996.0	
germarium maximum width	62.6–149.1	62.6–141.9			48.7–92.9	
seminal receptacle length	55.0–532.6	72.6			52.4–110.9	
seminal receptacle width	56.1–620.1	115.9			64.8–159.8	
vitellaria to anterior end distance	229.0–627.1	436.3–774.4			402.3–571.0	
length of vitellaria within haptor	1.1–61.5	57.3–102.8			21.6–140.1	
distance between vitellaria posterior limbs	0.0–204.8	0.0			0.0	
left efferent vitelline duct length	142.7–659.8	248.4–361.1			148.5–601.1	
right efferent vitelline duct length	124.2–963.2	150.2–330.9			146.9–590.7	
deferent vitelline duct length	114.1–419.2	139.4–262.7			156.8–317.5	
egg length (without filaments)	162.3–219.5	–			–	215–257
egg width (without filaments)	58.5–92.2	–			–	50–85
abopercular filament length	63.6–169.8	–			–	

MAFFT v.7 (Katoh & Standley, 2013) under default gap parameters on the European Molecular Biology Laboratory–European Bioinformatics Institute bioinformatics web platform (<http://www.ebi.ac.uk/Tools/msa/mafft>) together with the currently available sequences for the *Microcotyle* species in the GenBank database (accessed on 25 June 2022; see table 4). The *cox1* alignment (396 nt) included a total of seven newly generated sequences and 17 published sequences from the ten species available on GenBank. *Bivagina pagrosomi* (Murray, 1931) Dillon & Hargis, 1965 ex *Sparus aurata* L. was used as an outgroup in analyses (Z83003) based on previous phylogenies of the group using this species as the outgroup (Ayadi et al., 2017; Nam et al., 2020; Villora-Montero et al., 2020; Lablack et al., 2022).

Model-based Bayesian inference (BI) and maximum likelihood (ML) analyses were carried out using MrBayes v.3.2.6 on XSEDE at the CIPRES Science Gateway v. 3.3 ([http://www.phylo.org/sub\\_sections/portal](http://www.phylo.org/sub_sections/portal)) (Miller et al., 2010) and PhyML v.3.0 (Guindon et al., 2010) on the ATGC bioinformatics platform (<http://www.atgc-montpellier.fr/>). BI analyses were run using Markov chain Monte Carlo chain searches on two simultaneous

runs of four chains for  $10^7$  generations, with trees sampled every  $10^3$  generations. The 'burn-in' was set for the first 25% of the trees sampled and consensus topology and nodal support was estimated from the remaining 75% of the trees. Posterior probabilities for the ML analyses were estimated with a non-parametric bootstrap validation of 1000 pseudoreplicates. Prior to both analyses the best-fitting models of nucleotide substitution were estimated under the Akaike information criterion using MEGA v 6. This was the Tamura–Nei model (Tamura et al., 2013) with gamma distributed among-site rate variation (TN93 +  $\Gamma$ ) for the ML, and the general time reversible model with gamma distributed among-site rate variation (GTR+  $\Gamma$ ) for the BI analysis. FigTree v.1.4.3 (Rambaut & Drummond, 2012) was used to visualize tree topologies. Posterior probabilities (PP) and bootstrap support (BS) values are summarized on the BI trees (as PP/BS). Distance matrices (uncorrected *p*-distance model) were calculated in MEGA v.6. Distance-based neighbour-joining analyses based on Kimura 2-parameter distances were also performed in MEGA v.6 with nodal support estimated using 1000 bootstrap replicates.

**Table 3.** Metrical data from descriptions of *Microcotyle* spp. similar to *Microcotyle merche* n. sp. from scorpenoid fishes.

Source	<i>Microcotyle sebastis</i>			<i>Microcotyle victoriae</i>	<i>Microcotyle caudata</i>				<i>Microcotyle neozealanicus</i>	<i>Microcotyle kasago</i>
	Goto, 1894	Yamaguti, 1934	Bonham & Guberlet, 1937	Woolcock, 1936	Goto, 1894	Yamaguti, 1934	Yamaguti, 1934	Ono et al., 2020	Dillon & Hargis, 1965	Ono et al., 2020
Host species	<i>Sebastes</i> spp.	<i>Sebastes schlegeli</i>	<i>Sebastes maliger</i> , <i>Sebastes caurinus</i> , <i>Sebastes melanops</i>	<i>Helicolenus percoides</i>	<i>Sebastes</i> spp.	<i>Sebastes inermis</i>	<i>Sebastes inermis</i>	<i>Sebastes ventriucosus</i> , <i>Sebastes cheni</i>	<i>Helicolenus percoides</i>	<i>Sebasticus marmoratus</i>
Locality	Japan Pacific	Japan Pacific	Pacific	Indian	Japan Pacific	Japan Pacific	Japan Pacific	Japan Pacific	Pacific	Japan Pacific
body length	5.500	3900–4100	3100–4600	3800–5400	3200	2440–2830	1800–2700	945–5550	1460–2920	1900–3550
body width		560–670	640–1050	700–1100		670–870	440–750	180–1400	460–770	360–720
haptor length			950–1700						560–1030	
number of clamps	58	52–56	46–62	34–50	50	60	32–52	27–69	48–58	20–44
clamp length	68–128			50–80	80			40–100	68–78	35–58
clamp width			88–117		45				47–54	50–80
sucker length			60–100	80–100				25–90	37–51	70–100
sucker width			54–95	60–80				30–80	44–59	63–98
pharynx length		45–48	52–81 <sup>a</sup>					20–90	44–62	53–75
pharynx width								20–100	47–61	23–75
oesophagus length										
testes to anterior end distance										
number of testes	40	36–43	21–48	18–22	23	20		4–24	11–20	10–14
genital atrium length								10–210	172–210	63–113
genital atrium width								40–250	177–256	65–108
Number of spines of the genital atrium			150–200							
length of spines in main chamber of the genital atrium			12 <sup>b</sup>	5–9	10			5–15	11	2.5–10

(Continued)

**Table 3.** (Continued.)

	<i>Microcotyle sebastis</i>			<i>Microcotyle victoriae</i>	<i>Microcotyle caudata</i>				<i>Microcotyle neozealanicus</i>	<i>Microcotyle kasago</i>
Source	Goto, 1894	Yamaguti, 1934	Bonham & Guberlet, 1937	Woolcock, 1936	Goto, 1894	Yamaguti, 1934	Yamaguti, 1934	Ono <i>et al.</i> , 2020	Dillon & Hargis, 1965	Ono <i>et al.</i> , 2020
Host species	<i>Sebastes</i> spp.	<i>Sebastes schlegeli</i>	<i>Sebastes maliger</i> , <i>Sebastes caurinus</i> , <i>Sebastes melanops</i>	<i>Helicolenus percoides</i>	<i>Sebastes</i> spp.	<i>Sebastes inermis</i>	<i>Sebastes inermis</i>	<i>Sebastes inermis</i> , <i>Sebastes ventriucosus</i> , <i>Sebastes cheni</i>	<i>Helicolenus percoides</i>	<i>Sebasticus marmoratus</i>
Locality	Japan Pacific	Japan Pacific	Pacific	Indian	Japan Pacific	Japan Pacific	Japan Pacific	Japan Pacific	Pacific	Japan Pacific
deferent vitelline duct length										
egg length (without filaments)			240				180	175–250	231–238	263
egg width (without filaments)			65					50–100	53–57	83

<sup>a</sup>Diameter.

<sup>b</sup>Length of the longest spine as indicated Bonham & Guberlet, 1937.



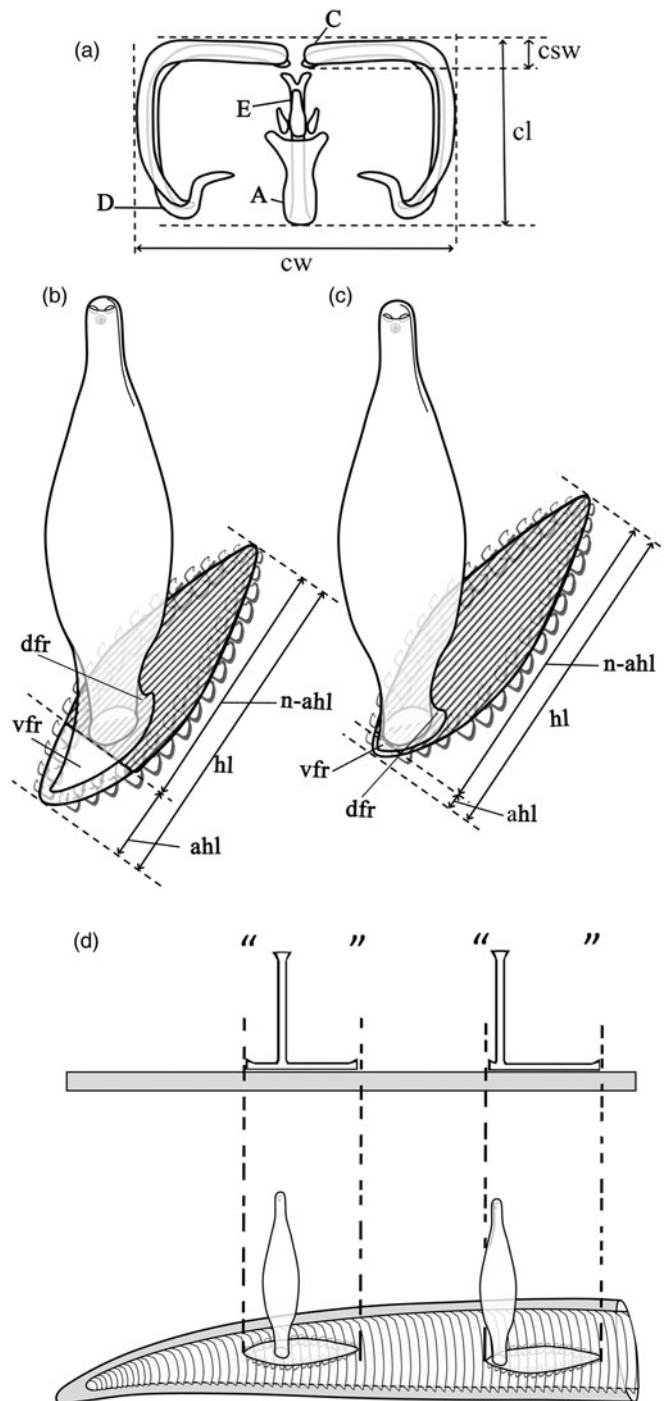


**Fig. 1.** Schematic representations for measurements of microcotylid clamps and haptors: (a) clamp measurements 'A', 'C', 'D' and 'E', microcotylid sclerites according to Llewellyn (1956); (b) and (c) unmounted specimens of *Microcotyle* sp., modified from fig. 1b in Villora-Montero *et al.* (2020)\* in three-dimensional (3D) ventrolateral views, (b) corresponds to the most habitual *Microcotyle* spp. haptor morphology, 'inverted T-shaped' (such as *Microcotyle merche* n. sp.) and (c) to 'L-shaped' haptor (such as *Microcotyle algeriensis*); and (d) body outlines of 'inverted T-shape' and 'L-shape' specimens of *Microcotyle* spp. in two-dimensional (up) and 3D (down) lateral views. Abbreviations: ahl, anterior haptor lobe length; cl, clamp length; cw, clamp width; csw, 'C' sclerite width; dfr, dorsal frenulum; hl, haptor length; n-ahl, haptor length without anterior lobe; and vfr, ventral frenulum. \*Note that the 'anterior haptor lobe' (ahl) is measured from the body-haptor junction to the anterior tip, and therefore 'the posterior haptor lobe length' (phl) in Villora-Montero *et al.* (2020) really corresponded to the length of the rest of the haptor (the haptor length without anterior lobe, 'n-ahl' in this figure).

## Results

### Molecular identification

Partial *cox1* sequences were generated from specimens recovered in the two fish hosts collected from the Western Mediterranean and north-east Atlantic coasts of Spain. Partial *cox1* (402–417 nt) sequences were generated for a total of seven isolates, that is, three *M. algeriensis* Ayadi, Gey, Justine & Tazerouti, 2016 ex *S. scrofa* collected from the north-east Atlantic and four *M. merche* n. sp. ex *H. dactylopterus* (two from the north-east Atlantic and two from the Western Mediterranean, see table 4). The newly generated *cox1* sequences were analysed together with 16 published sequences for *Microcotyle* spp. using *Bivagina pagrosomi* (GenBank: Z83003; Littlewood *et al.*, 1997) as an outgroup (table 4). The tree resulting from the BI analysis is provided in fig. 2 together with the statistical support from the ML analysis. The seven newly generated isolates clustered together with high support with the isolates of *M. algeriensis* ex *S. notata* (GenBank: KX926443; Ayadi *et al.*, 2017) and *Microcotyle* sp. ex *H. dactylopterus* (GenBank: KX926447; Ayadi *et al.*, 2017), reported from the southern coast of the Western Mediterranean off Algeria. The three isolates ex *S. scrofa* clustered together with the isolate of *M. algeriensis* ex *S. notata* (Ayadi *et al.*, 2017), while the sequences for the four isolates of *M. merche* n. sp. ex *H. dactylopterus* from the north-east Atlantic and the Western Mediterranean clustered together with the published sequences for *Microcotyle* sp. from the same host species (Ayadi *et al.*, 2017), albeit with poor support for both groupings. Overall, the *cox1* phylogeny (fig. 2) recovered a well-supported group of species of *Microcotyle* collected from hosts of the family Sebastidae: *Microcotyle caudata* Goto, 1894 ex *Sebastes inermis* Cuvier, 1829; *Microcotyle kasago* Ono *et al.*, 2020 ex *Sebastes marmoratus* (Cuvier, 1829); and *M. sebastis* Goto, 1894 ex *Se. schlegelii* Hilgendorf, 1880. Although with poor support, this group was also clustered together with the group formed by the newly generated sequences of *M. algeriensis* ex *S. notata* and *Microcotyle* sp. ex *H. dactylopterus*.

The intraspecific sequence divergence (see Online Supplementary Table S1) between the newly generated *cox1* sequences for *M. algeriensis* (ex *S. scrofa*) was 0.2% (1 nt difference), while the two sequences for *M. merche* n. sp. from the north-east Atlantic and the Western Mediterranean were identical. The newly generated sequences for the isolates of *M. algeriensis* ex *S. scrofa* from the north-east Atlantic differed by 3.8–4.0% (15–16 nt) from *M. algeriensis* ex *S. notata* from off of Algeria; the sequences for *M. merche* n. sp. ex *H. dactylopterus* differed by 4.5–5.3% (18–21 nt) from the published isolate of *M. algeriensis* ex *S. notata* from off of Algeria. The newly generated isolates of *M. merche* n. sp. ex *H. dactylopterus* differed from *Microcotyle* sp. ex *H. dactylopterus* from off of Algeria by 0.8–2.5% (3–10 nt) and by 2.8–3.8% (11–16 nt) from *M. algeriensis* ex *S. scrofa* from the north-east Atlantic. The newly generated isolates of *M. merche* n. sp. ex *H. dactylopterus* from the north-east Atlantic differed from the Western Mediterranean by 2.3% (9 nt difference). The overall interspecific sequence divergence for the genus *Microcotyle* ranged between 8.1–16.4% (31–65 nt difference).

### Taxonomic summary

Family: Microcotylidae Taschenberg, 1879

Subfamily: Microcotylinae Taschenberg, 1879

*Microcotyle merche* n. sp. ex *Helicolenus dactylopterus*

**Table 4.** Summary data for the isolates of *Microcotyle* spp. used in the phylogenetic analyses.

Parasite species	Host species	United Nations Food and Agriculture Organization Fishing Areas	GenBank Identification	Source
<i>Microcotyle merche</i> n. sp.	<i>Helicolenus dactylopterus</i>	WM	<b>OQ243286</b>	present study
			<b>OQ243287</b>	
		NEA	<b>OQ243284</b>	
			<b>OQ243285</b>	
<i>Microcotyle algeriensis</i>	<i>Scorpaena notata</i>	WM	KX926443	Ayadi et al. (2017)
		NEA	<b>OQ243288</b>	present study
			<b>OQ243289</b>	
<i>Microcotyle caudata</i>	<i>Sebastes inermis</i>	NWP	MW730633	Nam et al. (2020)
			MW730636	
<i>Microcotyle erythrini</i>	<i>Pagellus erythrinus</i>	WM	MN816012	Villora-Montero et al. (2020)
	<i>Pagrus pagrus</i>	WM	MN816017	
<i>Microcotyle isyebi</i>	<i>Boops boops</i>	WM	MN816019	
			MN816021	
<i>Microcotyle kasago</i>	<i>Sebastes marmoratus</i>	NWP	LC472526	Ono et al. (2020)
<i>Microcotyle sebastis</i>	<i>Sebastes schlegelii</i>	NWP	MT876115	Song et al. (2021)
			MT876116	
<i>Microcotyle</i> sp. DG-2016	<i>Helicolenus dactylopterus</i>	WM	KX926447	Ayadi et al. (2017)
<i>Microcotyle visa</i>	<i>Pagrus caeruleostictus</i>	WM	MK275652	Bouguerche et al. (2019a)
			MK275654	
<i>Microcotyle whittingtoni</i> n. sp.	<i>Dentex dentex</i>	WM	MN816010	Villora-Montero et al. (2020)
			MN816011	
'Paramicrocotyle' sp. FAS-2014	<i>Pinguipes chilensis</i>	SWP	KJ794215	Oliva et al. (2014)
outgroup				
<i>Bivagina pagrosomi</i>	<i>Sparus aurata</i> <sup>a</sup>	SWP	Z83003	Littlewood et al. (1997)

Abbreviations: NEA, north-east Atlantic; NWP, north-west Pacific; SA, southern Australia; SWP, south-west Pacific; WM, Western Mediterranean.

Note: The newly generated sequences are indicated in boldface type.

<sup>a</sup>As *Sparus auratus* in Littlewood et al. (1997).

Type host: Blackbelly rosefish, *H. dactylopterus* (Teleostei: Sebastidae) [weight: 27.7–338.9 (94.2 ± 72.5); standard length: 10.5–19.5 (14.0 ± 2.6)] off Guardamar del Segura, Spain; [weight: 327.0–507.5 (403.6 ± 52.8); standard length: 22.4–26.5 (25.0 ± 1.0)] in Bay of Biscay, Spain.

Type locality: Off Guardamar del Segura, Western Mediterranean off Spain. Other localities with valid records: Bay of Biscay off Spain; off Bouharoun, Algeria; and off Montenegro.

Site of infection: Gill filaments.

Infection parameters: Off Guardamar del Segura, Spain ( $n = 74$ ): prevalence, 24% (18 out of 74); mean intensity, 2.17 ± 1.95; Bay of Biscay off Spain ( $n = 33$ ): prevalence, 52% (17 out of 33); mean intensity, 1.76 ± 1.20.

Deposition of specimens: Holotype (2023.2.2.1) and three paratypes (2023.2.2.2–2023.2.2.4) (from Guardamar del Segura, and from Guardamar del Segura and the Bay of Biscay, respectively) deposited at the NHMUK; remaining material from Guardamar del Segura and Bay of Biscay deposited in the parasitological

collection of the Cavanilles Institute of Biodiversity and Evolutionary Biology, University of Valencia, Spain.

Molecular sequence data: GenBank accession numbers: OQ243284–OQ243287 (*cox1*).

ZooBank registration: urn:lsid:zoobank.org:act:40CFA7F5-4465-4FAD-993F-C39FC2A95649

Comparative specimens examined: Five vouchers ex *H. dactylopterus* from Bouharoun, Algeria, deposited at the Muséum National d'Histoire Naturelle, Paris (MNHN HEL579 A–E).

Etymology: The new species is named in apposition, in honour of the Dr Mercedes Fernández ('Merche'), from the University of Valencia, an eminent biologist, and an expert in aquatic animal parasitology. Mercedes Fernández has taught and inspired several generations of biologists and parasitologists thanks to her talent and selfless dedication.

Description

Based on 40 mature adults, (20 ex *H. dactylopterus* from the Western Mediterranean and 20 from the north-east Atlantic),



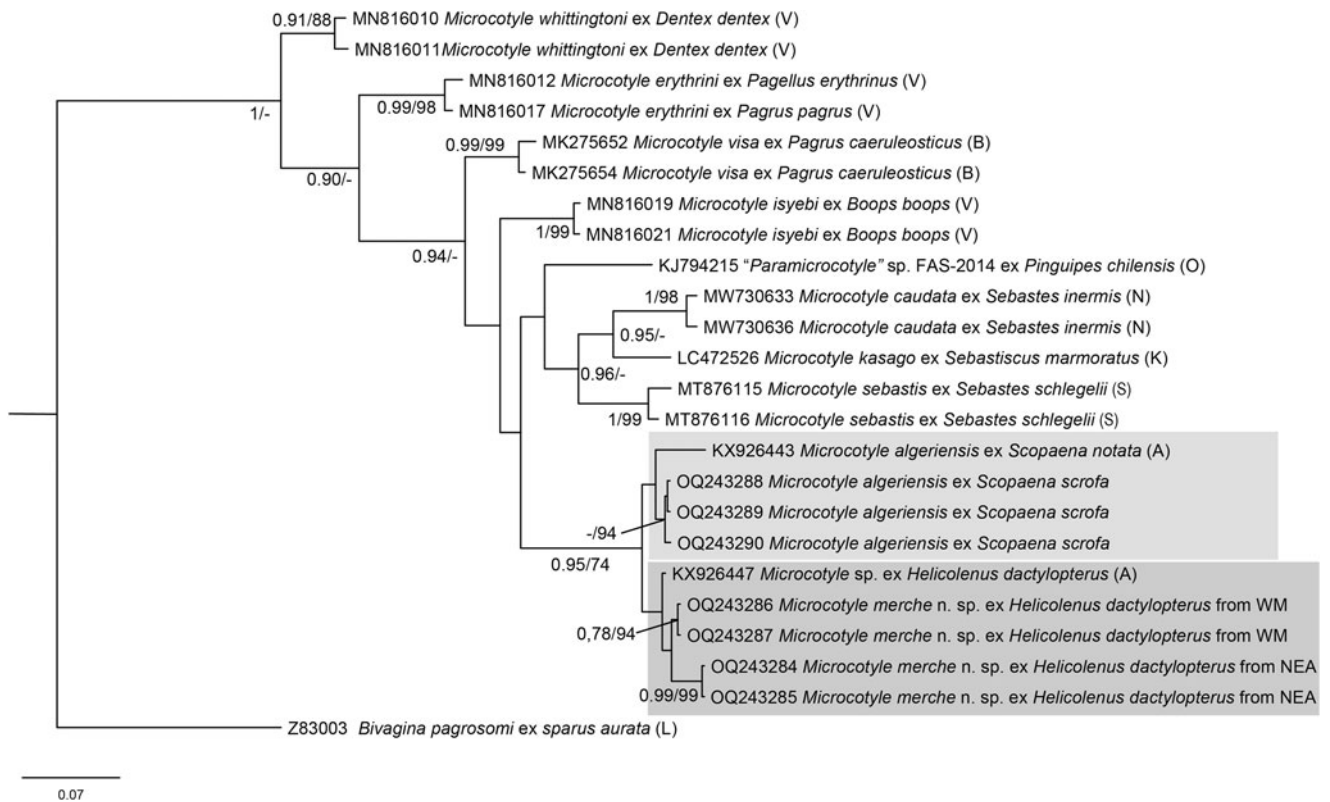


**Fig. 2.** Bayesian inference (BI) phylogram based on the mitochondrial cytochrome c oxidase subunit 1 gene dataset for *Microcotyle* spp. *Bivagina pagrosomi* was used as an outgroup. Posterior probabilities and bootstrap support values are shown as nodal support; only values > 0.90 (BI) and 75% (maximum likelihood). The scale-bar indicates the expected number of substitutions per site. Sequence identification is as in GenBank, followed by a letter: A, Ayadi *et al.* (2017); B, Bouguerche *et al.* (2019a); K, Ono *et al.* (2020); L, Littlewood *et al.* (1997); N, Nam *et al.* (2020); O, Oliva *et al.* (2014); S, Song *et al.* (2021); and V, Villora-Montero *et al.* (2020). Geographical abbreviations: NEA, north-east Atlantic; and WM, Western Mediterranean.

except when otherwise indicated. Morphometric data refer to specimens from both localities together; ranges (when more than one specimen was measured) are provided in table 2, including measurements from specimens from each locality separately; see fig. 3.

Body fusiform, elongate, occasionally slender,  $3963.4 \pm 740.3$  long and  $173.0 \pm 39.4$  wide at level of suckers,  $314.3 \pm 68.5$  wide at level of genital atrium,  $612.8 \pm 159.4$  wide at level of germarium (maximum width), and  $449.4 \pm 125.0$  wide at level of testes.

Haptor elongated, spatulate, pointed at anterior and posterior extremities, well differentiated from body (haptor length/total length ratio 20–37% (30%)), peduncle inconspicuous; laterally symmetrical, divided into an anterior (ventral) lobe and a longer posterior (dorsal) lobe (anterior/posterior haptor lobe length ratio 10–38% (19%) ( $n = 30$ )) (see figs 1b and 3). A ventral frenulum connects the anterior haptor lobe with the body ventral surface and a small dorsal frenulum connects the posterior lobe with the body dorsal surface (fig. 1b). Haptor clamps in two laterals frills, sessile or slightly protruded, in two rows (42–60 in total number; 8–14 in the anterior haptor projection). Clamps ‘microcotylid’ type, relative robust (‘C’ sclerite maximum width  $5.3 \pm 1.0$  and  $0.105 \pm 0.021$  corrected by clamp length ( $n = 54$ )); trident-shaped accessory sclerite (‘E’) with long thick central bar reaching to distal tips of the antero-lateral sclerites ‘C’ and two delicate lateral branches originating at the base of ‘E’. Clamps at the anterior and posterior ends of the haptor slightly smaller.

Mouth subventral within subconical vestibule with a pair of septate buccal suckers ventrally oriented. Pharynx muscular,

subspherical; oesophagus short, connected to intestinal bifurcation at the end or posterior to the genital atrium. Caeca mostly pre-haptoral, ramified with the vitellaria in inner and external lateral branches (external more profuse).

Testes flattened, irregular, numerous (13–22 in number), arranged in clusters of 1–2 rows, and some testes piled up dorsally or ventrally; testicular field at  $2092.2 \pm 503.5$  from anterior extremity of the body, post-germarial and pre-haptoral. Testes area ending up to  $549.5 \pm 150.1$  from the insertion of the haptor. Vas deferens wide, straight, dorsal to the uterus, ending in a short muscular copulatory organ ( $55.8 \pm 13.5 \times 50.7 \pm 13.0$  ( $n = 11$ )) posterior to genital atrium. Genital atrium at  $262.5 \pm 108.8$  from anterior end, formed by a wide medial muscular chamber, armed with small conical spines (146–221 in number), followed by two posterior small lateral chambers (‘pockets’ *sensu* Mamaev, 1989) one on each side of the copulatory organ ( $41.2$ – $85.3$ ,  $n = 10$ ). Pockets armed with conical spines (23–40 in number, 24 in holotype), longer than the ones in the main chamber (see table 2).

Germarium at  $1770.8 \pm 320.4$  ( $n = 34$ ) from anterior end;  $884.3 \pm 239.7$  long ( $n = 25$ ), question mark-shaped; proximal globular germinal area  $134.1 \pm 45.8 \times 113.7 \pm 32.6$  ( $n = 31$ ) followed by a straight section  $351.5 \pm 113.4$  ( $n = 31$ ), widening in a long distal globular region  $532.8 \pm 147.4$  long ( $n = 25$ ) with a proximal arched dextro-sinistral section, connected to a wider distal arch directed sinistro-dextrally, with a maximum distal width of  $88.5 \pm 24.0$  ( $n = 27$ ). Oviduct slightly sinuous, including an elongated seminal receptacle  $244.7 \pm 178.4 \times 211.6 \pm 187.0$  ( $n = 9$ ) directed postero-sinistrally; ending in an oötype, with Mehlis’

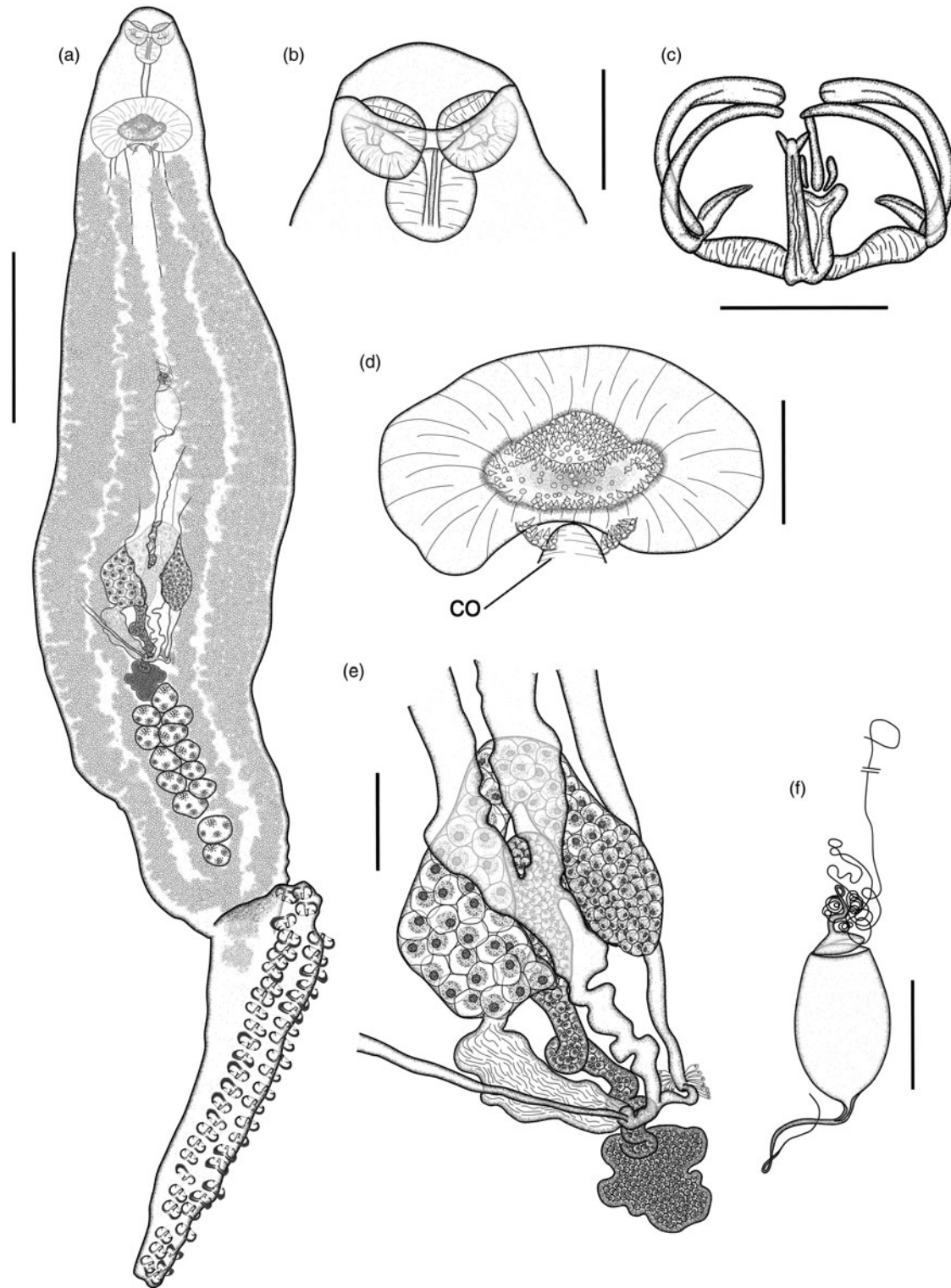


**Fig. 3.** *Microcotyle merce* n. sp. from *Helicolenus dactylopterus* (Delaroche, 1809) from Guardamar del Segura, Spain. All drawings from the holotype: (a) whole mount; (b) anterior body end; (c) clamp; (d) genital atrium, including copulatory organ; (e) germarium; and (f) egg. Scale bars: (a) 500  $\mu$ m; (b), (d)–(f) 100  $\mu$ m; (c) 50  $\mu$ m.

gland. Uterus ascending straight with curving walls, ending in genital atrium.

Vaginal pore unarmed, mid-dorsal, often unobserved, at  $1087.7 \pm 426.6$  from anterior end ( $n = 8$ ). Vitelline follicles disperse, posterior or overlapping with genital atrium, starting at

$481.4 \pm 127.0$  from anterior body extremity, extended in lateral fields surrounding caecal ramifications and surrounding the testes, usually pre-haptoral ( $n = 33$ ). Posterior fields of vitellaria mostly joined ( $n = 38$ ), with one single specimen with different field lengths (204.8). Vitelline ducts Y-shaped, with two unjoined

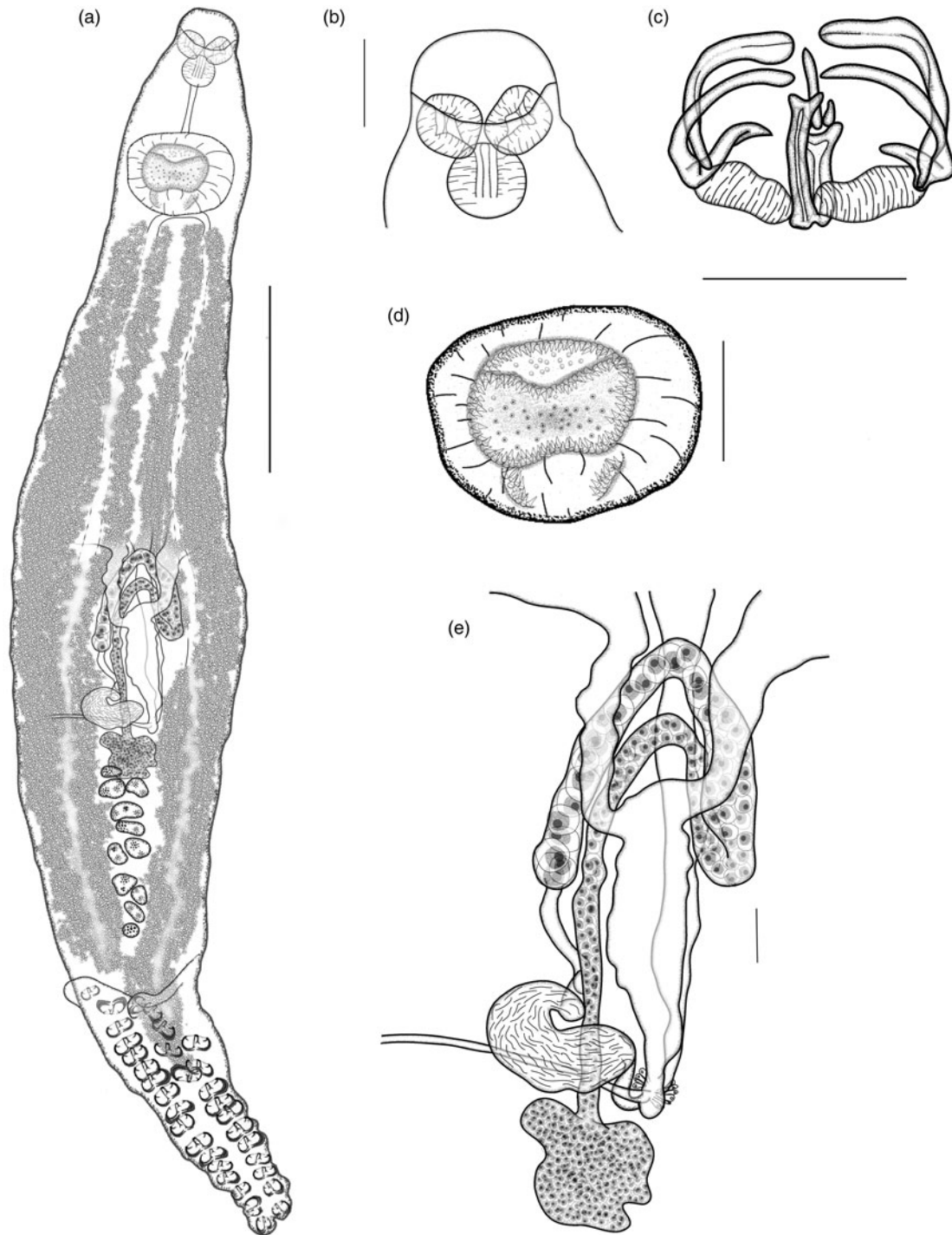


**Fig. 4.** *Microcotyle algeriensis* Ayadi, Gey, Justine & Tazerouti, 2016, from *Scorpaena scrofa* L. from Guardamar del Segura, Spain. All drawings from the same voucher specimen: (a) whole mount; (b) anterior body end; (c) clamp; (d) genital atrium; and (e) germarium. Scale bars: (a) 500  $\mu$ m; (b), (d)–(f) 100  $\mu$ m; (c) 50  $\mu$ m.

ducts  $300.6 \pm 174.0$  and  $366.3 \pm 145.4$  long (right and left, respectively) ( $n = 26$ ), joining ventral to the germarium in a slightly sinuous deferent duct,  $240.8 \pm 78.3$  long ( $n = 26$ ).

Egg fusiform; opercular filament long and thin and abopercular filament short and thin. Operculum with hollow tip, abruptly narrowed into a tubular section continuing into a solid opercular filament. Filaments' tips solid and either not capitated or slightly capitated.

#### Remarks

Five species of *Microcotyle* are known to parasitize sebastids (*M. caudata* (syn. *Microcotyle sebastisci* Yamaguti, 1958), *M. kasago*, *Microcotyle neozealanicus* Dillon & Hargis, 1965, *M. sebastis* and *Microcotyle victoriae* Woolcock, 1936), and all of them have been described from Pacific fishes, for example, *M. caudata*, *M. neozealanicus* and *M. victoriae* in *Helicolenus* spp. Additionally, Balboa & Nascimento (1998) reported *Microcotyle*



sp. ex *Helicolenus lengerichi* Norman, 1937 (and *Sebastes capensis* (Gmelin, 1789)) off of Chile, although no morphological information was provided. According to the numbers of clamps and testes, *M. merche* n. sp. mostly resembles *M. kasago* from *Seb. marmoratus* and *M. neozelanicus* and *M. victoriae*, both from *Helicolenus percooides* (Richardson & Solander, 1842) (see table 3). These traits marginally overlap in *M. merche* n. sp. and *M. kasago* and overlap with *M. neozelanicus* and *M. victoriae*. Other diagnostic traits such as the number of spines of the genital atrium are not reported in these species' descriptions; however, this region is graphically represented in all these descriptions. Counts conducted from original drawings reveal differences in the number of spines of the lateral small chambers of *M. merche* n. sp. (24–39), higher than those of *M. kasago* (14), *M. neozelanicus* (21) and *M. victoriae* (22).

Two records of *Microcotyle* sp. have been reported in Mediterranean *H. dactylopterus*: off of Montenegro (Radujković & Euzet, 1989, as *M. sebastis*) and Algeria (Ayadi et al., 2017, as *Microcotyle* sp.). These exemplars must be considered as *M. merche* n. sp. as their traits fit with the present description (see table 2), therefore expanding the distribution of the new species to the north-central and south-western Mediterranean. The re-examination of the vouchers of *Microcotyle* sp. from Algerian *H. dactylopterus* also revealed no incongruence with the description of *M. merche* n. sp. Another species, *M. algeriensis* has been reported in other Mediterranean scorpaenoid fishes (Scorpaenidae): *S. notata* off Algeria (Ayadi et al., 2017); and *S. scrofa* from the Bay of Biscay (present study). *Microcotyle algeriensis* can be differentiated from the new species by the lower number of clamps (22–39 vs. 42–60 in *M. merche* n. sp.). Moreover, the haptor shape of *M. algeriensis* is characterized by its uniquely short anterior lobe (or absent, see remarks on *M. algeriensis* below and fig. 1).

The new species can also be distinguished from other Mediterranean species, many of them parasites of sparids (*Microcotyle erythrini* Van Beneden & Hesse, 1863, *Microcotyle isyebi* Bouguerche, Gey, Justine & Tazerouti, 2019, *Microcotyle visa* Bouguerche, Gey, Justine & Tazerouti, 2019 and *Microcotyle whittingtoni* Villora-Montero, Pérez-del-Olmo, Georgieva, Raga & Montero, 2020, see Online supplementary Table S3 in Villora-Montero et al., 2020), but also in fishes from other families (*Microcotyle donavini* Van Beneden & Hesse, 1863, *Microcotyle lichiae* Ariola, 1899 and *Microcotyle pomatomi* Goto, 1899, see supplementary table S4 in Villora-Montero et al., 2020). The number of clamps of *M. merche* n. sp. (42–60) is smaller than those of these species except for *M. lichiae* (52); however, the body length of this latter species (8000) is much greater than the body length of this new species (2517–5706). *Microcotyle isyebi* and *M. visa* are similar to *M. merche* n. sp., and the number of clamps slightly overlaps (54–102 and 59–126, respectively). The ranges of number of clamps of these species required re-examination, as they are particularly wide, especially regarding the lower values; in fact, Villora-Montero et al. (2020) reported a much narrower range of clamps number in their description of *M. isyebi* from Spanish specimens (80–100), which does not overlap with that of the new species.

#### Taxonomic summary

##### *M. algeriensis* ex *S. scrofa*

**Host:** Red scorpionfish, *S. scrofa* (Teleostei: Scorpaenidae) (weight: 292.5–745.1 (542.6 ± 123.7); standard length: 23.5–29.3 (26.2 ±

2.0)) (new host), other hosts with valid records *S. notata* (Teleostei: Scorpaenidae) (type-host).

**Locality:** Bay of Biscay off Spain. Other localities with valid records: off Bouharoun, Algeria (type-locality).

**Site of infection:** Gill filaments.

**Infection parameters:**  $n = 19$ ; prevalence, 58% (11 out of 19); mean intensity, 4.09 ± 2.61.

**Deposition of specimens:** Two specimens from Bay of Biscay off Spain are deposited in the NHMUK (2023.2.2.5–2023.2.2.6); remaining material from Bay of Biscay in the parasitological collection of the Cavanilles Institute of Biodiversity and Evolutionary Biology, University of Valencia, Spain.

**Molecular sequence data:** GenBank accession numbers: OQ243288–OQ243290 (*cox1*).

##### Description

Based on 19 mature adults; ranges (when more than one specimen was measured) are provided in table 2; fig. 4.

Body fusiform and elongate, often slender, 3173.9 ± 633.2 long and 164.0 ± 15.9 wide at level of suckers, 292.8 ± 29.9 wide at level of genital atrium, 548.2 ± 99.1 wide at level of germarium (maximum width), and 410.2 ± 81.5 wide at level of testes.

Haptor flat and spindle-shaped, well differentiated from the body (haptor length/total length ratio 15–59% (27%)), peduncle not visible; laterally symmetrical, projected in a very short anterior (ventral) lobe (often not distinguishable) and a relatively longer posterior (dorsal) lobe (anterior/posterior haptoral lobe length ratio 0–9% (5%) ( $n = 16$ )). Two small frenula connect anterior and posterior haptor lobes with ventral and dorsal body surfaces, respectively (see fig. 1c). Haptor with two lateral frills armed each with one row of sessile or slightly protruded clamps (22–34 in total number; 0–4 in the anterior projection). Clamps 'microcotylid' type, robust ('C' sclerite maximum width 3.9 ± 0.9 and 0.092 ± 0.020 corrected by clamp length ( $n = 29$ )); trident-shaped accessory sclerite 'E' formed by long thick central bar reaching to distal tips of the antero-lateral sclerites 'C' and two lateral slender and short bars originating at the base of 'E'. Clamps at the anterior and posterior ends of the haptor smaller.

Mouth ventro-subterminal, within a funnel-shaped vestibule including a pair of septate buccal suckers. Muscular pharynx sub-spherical, followed by a short oesophagus; intestine bifurcation at the end of the genital atrium. Caeca usually not extending within the haptor, with inner and external lateral ramifications accompanying vitellaria; external branches more profuse.

Testes flattened and irregular (7–10 in number), arranged in 1–2 rows, with some testes piled up; testicular field at 1872.9 ± 192.6 ( $n = 16$ ) from anterior extremity of the body; testes post-germarial and pre-haptoral. Testicular area ends up to 525.3 ± 254.6 ( $n = 17$ ) from the insertion of the haptor. Vas deferens wide, unwinding, dorsal to uterus; muscular copulatory organ short (45.8 ± 8.1 × 52.9 ± 5.1 ( $n = 3$ )), protruded at the posterior part of the genital atrium. Genital atrium at 300.1 ± 28.9 from anterior extremity of the body, formed by a main wide medial armed muscular chamber, armed with small conical spines (189–234 in number), connected to two small postero-lateral chambers (pockets), at either side of the copulatory organ (39.6–55.0,  $n = 3$ ). Pockets with conical spines (20–38 in number), longer than the main chamber spines (see table 2).

Germarium 743.1 ± 119.8 long ( $n = 15$ ), at 1795.4 ± 179.6 ( $n = 15$ ) from anterior end; question mark-shaped with proximal globular germinal area 113.9 ± 22.4 × 110.2 ± 38.0 ( $n = 14$ ) connected to a straight and narrow section 306.6 ± 77.0 ( $n = 31$ ), widening into a tubular region 436.5 ± 72.7 long ( $n = 14$ ) with a

proximal arched dextro-sinistral section, connected to a wider distal arch directed sinistro-dextrally, with a maximum distal width of  $67.6 \pm 15.0$  ( $n = 14$ ). Oviduct, directed postero-sinistrally, with an elongated oviducal seminal receptacle  $76.3 \pm 30.7 \times 110.1 \pm 47.6$  ( $n = 5$ ) joined to the oötype by a sinuous narrow section. Oötype with Mehlis' gland well developed. Uterus wide, ascending straight up to the genital atrium.

Vaginal pore unarmed, medial, dorsal, observed in one specimen at 238.6 from anterior extremity of the body. Vitelline follicles disperse, posterior or overlapping with genital atrium, spread from  $495.3 \pm 41.8$  from anterior extremity of the body, extended in lateral fields together with the caeca and surrounding the testes, on occasion pre-haptoral ( $n = 17$ ). Posterior fields of vitellaria always joined ( $n = 17$ ). Vitelline ducts Y-shaped, with two unjoined ducts  $327.5 \pm 118.0$  and  $345.2 \pm 121.6$  long (right and left, respectively) ( $n = 11$ ), joining ventral to germarium in a slightly sinuous deferent duct,  $227.0 \pm 39.8$  long ( $n = 11$ ). No eggs observed.

#### Remarks

The specimens of *M. algeriensis* ex *S. scrofa* from the Spanish Atlantic share the same morphological and molecular traits of the specimens originally described ex *S. notata* off Algeria (Ayadi *et al.*, 2017). This species has not been found in *S. notata* from the Spanish Mediterranean (neither in *S. porcus* from Spain). Based on the new specimens analysed in this study, some comments on relevant diagnostic characters regarding the haptor of *M. algeriensis* must be pointed out. According to the original description the haptor is 'continuous with body', however, as in other *Microcotyle* species, the body is inserted perpendicularly to a haptor projected into two lobes, one ventral and one dorsal (see fig. 1c). A distinctive trait of *M. algeriensis*, previously unreported in other *Microcotyle* species, is the short or almost absent ventral lobe (this trait also differentiates *M. merche* n. sp. from *M. algeriensis*, see schematic comparative drawings in fig. 1b, c). Subsequently the haptor is slightly short and the number of clamps of this species is inferior to other *Microcotyle* spp. (see tables 2 and 3). Another minor comment regards the number of spines of the main chamber of the genital atrium, slightly higher in the specimens' ex *S. scrofa* than in the species description. Unfortunately, type specimens are not available, and a recount of the genital atrium spines was not possible.

## Discussion

This study increases the knowledge about the diversity of species of *Microcotyle* within the Scorpaenidae, specifically in scorpaenids and sebastids. Interestingly, *M. algeriensis* and *M. merche* n. sp. are not only geographically, but also phylogenetically close. This finding is particularly interesting as several authors consider that sebastids should be included in a subfamily (Sebastinae) within the Scorpaenidae (Jia *et al.*, 2020). In fact, the genetic distance between *M. algeriensis* and *M. merche* n. sp. is very narrow, although the prominently distinct morphology (including key diagnostic traits as clamp number, haptor dimensions or genital atrium spines) and the phylogenetic tree clearly differentiate both species. In contrast, other more genetically distant species, such as *M. caudata*, are highly difficult to differentiate morphologically from these species (particularly from *M. merche* n. sp.).

The description of *M. merche* n. sp. contributes to the delimitation of the host and geographical distribution of *M. sebastis*, a species which has mostly reported in sebastids (in up to 40 species of *Sebastes*), but there are also several doubtful reports worldwide in species of non-sebastid fishes such as aulorhynchids,

paralichthyids and syngnathids (Gibson *et al.*, 2006). According to the present study the specimens of *M. sebastis* reported by Radujković & Euzet (1989) in Mediterranean *H. dactylopterus* are in fact *M. merche* n. sp., thus meaning that *M. sebastis* is not present in this sea. Furthermore, the high number of historical reports indicate that *M. sebastis* is probably specific to species of *Sebastes* Cuvier, 1829 from the Pacific Ocean, and that other host and locality reports should be re-examined (Gibson *et al.*, 2006). This work also expands the reported host range and geographical distribution of *M. algeriensis*. Interestingly, neither this species nor any other microcotylid species has been found in the other *Scorpaena* species analysed in this study (the type host *S. notata* and *S. porcus*), despite the fact that these fishes are sympatric and the localities are relatively close to Algeria. These local differences can be explained by the high sedentarism of the species of the *Scorpaena* genus (Hureau & Litvinenko, 1986). In *S. porcus* from Italy, Ulmer & James (1981) found *M. cf. sebastisci*, which according to Ono *et al.* (2020) was a possible synonym of *M. caudata* due to misidentification; however, based on the similarities in host genus, distribution and morphology, these specimens could also be *M. algeriensis*.

As indicated by Villora-Montero *et al.* (2020) the haptors of the species of *Microcotyle* are arranged in a three-dimensional pattern, usually undescribed or wrongly interpreted based on the two-dimensional way of mounting the specimens. Figure 1 in Villora-Montero *et al.* (2020) describes the haptor morphology in three-dimensions, including the parts to be measured in order to compare species. With the aim of standardizing the way of measuring the haptor lobes and avoiding the overlap of the body and haptor in mounted specimens, a modified version of the figure is herein included (fig. 1b, c); both dorsal and ventral lobes of the haptor are herein measured from their tips to their connection to the body, not from their tips to the centre of the insertion of the body, as this point is often difficult to identify. These standardized measures are useful to describe objectively (numerically) the short ventral lobe of *M. algeriensis* (table 2). The arrangement of the haptor of this species is unique (previously undescribed so far), as the ventral lobe is almost indistinct or absent, giving the worm an 'L-shape' in lateral view, instead of an 'inverted T-shape' (fig. 1d), with anterior and posterior projections perpendicular to the body. This trait could exist in other *Microcotyle* species, but it could have gone unseen, especially in mounted individuals, where the anterior part of the haptor usually overlaps with the body. *Microcotyle merche* n. sp. shows the habitual arrangement of the haptor with distinct ventral and dorsal projection ('inverted T-shape', fig. 1d) as seen in other *Microcotyle* species (see also Villora-Montero *et al.*, 2020). Haptor shape is not only relevant taxonomically, but also functionally, as the 'L-shape' haptor lacks the extra ventral clamps of the anterior projection lobe. These anterior clamps would contribute to parasite attachment, not only increasing the number of anchoring points, but also improving the antero-posterior balance, something crucial in this type of gill monogeneans, ectoparasites that can stretch their elongated bodies to reach distant parts of the branchial region (Buchmann & Bresciani, 2006).

Eleven species of Scorpaenidae and Sebastidae exist in the Mediterranean (World Register of Marine Species, 2022), six of them *Scorpaena* spp., and specimens of four of them have been analysed to date (Radujković & Euzet, 1989; Ayadi *et al.*, 2017; present study), showing very interesting differences in the diversity of *Microcotyle* spp. of hosts from relatively close geographical

areas of this sea. Knowing more about the diversity of *Microcotyle* spp. in the Mediterranean ecosystem can provide not only relevant information on the taxonomy and phylogeny of *Microcotyle* spp. within scorpaenoids, but also on these hosts' distribution and biology.

**Supplementary material.** To view supplementary material for this article, please visit <http://doi.org/10.1017/S0022149X23000019>.

**Acknowledgements.** The authors thank Dr David I. Gibson (Natural History Museum, UK) for his generous advice on taxonomy and nomenclature and Dr Jean-Lou Justine (Muséum National d'Histoire Naturelle, France) for his generous comments and the loan of specimens. We are indebted to Rachel V. Pool (University of Valencia) for revising the English and to the anonymous reviewers for their helpful comments and suggestions.

**Financial support.** This work was supported by the Spanish Government [project MINECO/FEDER PID2019-110730RB-I00] co-funded by the Spanish Ministry for Science and Innovation (MCIN) MCIN/AEI/10.13039/501100011033 by 'ERDF A way of making Europe' by the European Union (EU), the Valencian Regional Government [project AICO/2021/279] and the ThinkInAzul programme supported by the MCIN with funding from the EU NextGenerationEU (PRTR-C17.I1), and by Generalitat Valenciana (THINKINAZUL/2021/029).

**Conflicts of interest.** None.

**Ethical standards.** Parasitological samples used in this study were collected from dead fish caught in the wild, that the fish species analyzed are not included in Royal Decree 139/2011 (BOE 2011), nor in the BOE 2020 of "Wild Species under Protection Regime Special and of the Spanish Catalog of Threatened Species", and that no additional permits are required in Spain to collect these organisms as they were originally destined for human consumption.

## References

- Ayadi ZEM, Gey D, Justine J and Tazerouti F (2017) A new species of *Microcotyle* (Monogenea: Microcotylidae) from *Scorpaena notata* (Teleostei: Scorpaenidae) in the Mediterranean Sea. *Parasitology International* **66**(2), 37–42.
- Balboa L and George-Nascimento M (1998) Variaciones ontogenéticas y entre años en las infracomunidades de parásitos metazoos de dos especies de peces marinos de Chile [Ontogenetic and inter-year variations in the infracommunities of metazoan parasites of two species of marine fish from Chile]. *Revista Chilena de Historia Natural* **71**(1), 27–37. [In Spanish.]
- Bonham K and Guberlet JE (1937) Notes on *Microcotyle sebastis* Goto from Puget Sound. *The Journal of Parasitology* **23**(3), 281–290.
- Bouguerche C, Gey D, Justine J and Tazerouti F (2019a) *Microcotyle visa* n. sp. (Monogenea: Microcotylidae), a gill parasite of *Pagrus caeruleostictus* (Valenciennes) (Teleostei: Sparidae) off the Algerian coast, Western Mediterranean. *Systematic Parasitology* **96**(2), 131–147.
- Bouguerche C, Gey D, Justine J and Tazerouti F (2019b) Towards the resolution of the *Microcotyle erythrini* species complex: description of *Microcotyle isyebi* n. sp. (Monogenea, Microcotylidae) from *Boops boops* (Teleostei, Sparidae) off the Algerian coast. *Parasitology Research* **118**(5), 1417–1428.
- Bowles J, Blair D and McManus DP (1995) A molecular phylogeny of the human schistosomes. *Molecular Phylogenetics and Evolution* **4**(2), 103–109.
- Buchmann K and Bresciani J (2006) Monogenea (Phylum Platyhelminthes). pp. 297–344. In Woo PTK (Ed.) *Fish diseases and disorders, volume 1*. Wallingford, CABI Publishing.
- Bush AO, Lafferty KD, Lotz JM and Shostak AW (1997) Parasitology meets ecology on its own terms: Margolis et al. revisited. *Journal of Parasitology* **83**, 575–583.
- Dillon WA and Hargis WJ (1965) Monogenetic trematodes from the southern Pacific Ocean: 2. Polyopisthocotyleids from New Zealand fishes: the families Discocotylidae, Microcotylidae, Axinidae, and Gastrocotylidae. *Biology of the Antarctic Seas II* **5**, 251–280.
- Gibson DI, Bray RA and Harris EA (Compilers) (2006) *Host-parasite database of the natural history museum*, London. Available at <https://www.nhm.ac.uk/research-curation/scientific-resources/taxonomy-systematics/host-parasites/> (accessed 23 November 2022).
- Goto S (1894) *Studies on the Ectoparasitic Trematodes of Japan*. Japan, Imperial University Tokyo. 183–95.
- Guindon S, Dufayard J, Lefort V, Anisimova M, Hordijk W and Gascuel O (2010) New algorithms and methods to estimate maximum-likelihood phylogenies: assessing the performance of PhyML 3.0. *Systematic Biology* **59**(3), 307–321.
- Hureau JC and Litvinenko NI (1986) Scorpaenidae. pp. 1211–1229. In Whitehead PJP, Bauchot ML, Hureau JC, Nielsen J and Tortonese E (Eds) *Fishes of north-eastern Atlantic and the Mediterranean, volume 3*. Paris, United Nations Educational, Scientific and Cultural Organization.
- Jia C, Zhang X, Xu S, Yang T, Yanagimoto T and Gao T (2020) Comparative analysis of the complete mitochondrial genomes of three rockfishes (Scorpaeniformes, *Sebastiscus*) and insights into the phylogenetic relationships of Sebastidae. *Bioscience Reports* **40**(12), BSR20203379.
- Katoh K and Standley DM (2013) MAFFT multiple sequence alignment software version 7: improvements in performance and usability. *Molecular Biology and Evolution* **30**(4), 772–780.
- Lablack L, Rima M, Georgieva S, Marzoug D and Kostadinova A (2022) Novel molecular data for monogenean parasites of sparid fishes in the Mediterranean and a molecular phylogeny of the Microcotylidae Taschenberg, 1879. *Current Research in Parasitology & Vector-Borne Diseases* **2**(1), 100069.
- Littlewood DTJ, Rohde K and Clough KA (1997) Parasite speciation within or between host species? Phylogenetic evidence from site-specific polystome monogeneans. *International Journal for Parasitology* **27**(11), 1289–1297.
- Llewellyn J (1956) The host-specificity, micro-ecology, adhesive attitudes, and comparative morphology of some trematode gill parasites. *Journal of the Marine Biological Association of the United Kingdom* **35**(1), 113–127.
- Mamaev YL (1986) The taxonomical composition of the family Microcotylidae Taschenberg, 1879 (Monogenea). *Folia Parasitologica* **33**(3), 199–206.
- Mamaev YL (1989) On species composition and morphological features of the *Microcotyle* genus (Microcotylidae, Monogenoidea). pp. 32–38. In Lebedev BI (Ed.) *Investigations in parasitology. Collection of papers*. Vladivostok, DBNTs AN SSSR. [In Russian.]
- Miller MA, Pfeiffer W and Schwartz T (2010) Creating the CIPRES Science Gateway for inference of large phylogenetic trees. pp. 1–8. In *Proceedings of the Gateway Computing Environments Workshop (GCE)*.
- Nam U, Whang I and Kim J (2020) The complete mitochondrial genome sequence of *Microcotyle caudata* (Platyhelminthes: Monogenea) from dark-banded rockfish (*Sebastes inermis*) in Korea. *Mitochondrial DNA Part B* **5**(2), 1817–1819.
- Oliva ME, Sepulveda FA and González MT (2014) *Parapedocotyle prolatili* gen. n. et sp. n., a representative of a new subfamily of the Didicoforidae (Monogenea), a gill parasite of *Prolatilus jugularis* (Teleostei: Pinguipedidae) from Chile. *Folia Parasitologica* **61**, 543.
- Ono N, Matsumoto R, Nitta M and Kamio Y (2020) Taxonomic revision of *Microcotyle caudata* Goto, 1894 parasitic on gills of sebastids (Scorpaeniformes: Sebastidae), with a description of *Microcotyle kasago* n. sp. (Monogenea: Microcotylidae) from off Japan. *Systematic Parasitology* **97**(5), 501–516.
- Pleijel F, Jondelius U, Norlinder E, Nygren A, Oxelman B, Schander C, Sundberg P and Thollesson M (2008) Phylogenies without roots? A plea for the use of vouchers in molecular phylogenetic studies. *Molecular Phylogenetics and Evolution* **48**(1), 369–371.
- Radujković BM and Euzet L (1989) Parasites of marine fishes of Montenegro: monogeneans. *Acta Adriatica* **30**(1–2), 51–135.
- Rambaut A and Drummond A (2012) *Figtree v1.4.0. Program package*. Available at <http://tree.bio.ed.ac.uk/software/figtree/> (accessed 24 March 2022).
- Schneider CA, Rasband WS and Eliceiri KW (2012) NIH image to ImageJ: 25 years of image analysis. *Nature Methods* **9**(7), 671–675.
- Song JY, Kim KY and Choi SW (2021) Occurrence and molecular identification of *Microcotyle sebastis* isolated from fish farms of the Korean rockfish, *Sebastes schlegelii*. *Korean Journal Parasitology* **59**(1), 89–95.



- Tamura K, Stecher G, Peterson D, Filipski A and Kumar S** (2013) MEGA6: molecular evolutionary genetics analysis version 6.0. *Molecular Biology and Evolution* **30**(12), 2725–2729.
- Ulmer MJ and James HA** (1981) Monogeneans of marine fishes from the Bay of Naples. *Transactions of the American Microscopical Society* **100**(4), 392–409.
- Van Beneden P and Hesse CE** (1863) Recherches sur les bdelloïdes ou hirudinés et les trématodes marins. *Mémoires de l'Académie Royale des Sciences, Brussels*, 1–142. [In French.]
- Villora-Montero M, Pérez-del-Olmo A, Georgieva S, Raga JA and Montero FE** (2020) Considerations on the taxonomy and morphology of *Microcotyle* spp.: redescription of *M. erythrini* van Beneden & Hesse, 1863 (*sensu stricto*) (Monogenea: Microcotylidae) and the description of a new species from *Dentex dentex* (L.) (Teleostei: Sparidae). *Parasites & Vectors* **13**(1), 1–23.
- Woolcock V** (1936) Monogenetic trematodes from some Australian fishes. *Parasitology* **28**(1), 79–91.
- World Register of Marine Species Database. WoRMS Editorial Board** (2022). An authoritative classification and catalogue of marine names. Available from <https://www.marinespecies.org> (accessed 23 November 2022).
- Yamaguti S** (1934) Studies on the helminth fauna of Japan. Part 2. Trematodes of fishes, I *Japanese Journal of Zoology* **5**, 267–269.